Infrared multiphoton decomposition of dimethylnitramine

ARTICLE *in* THE JOURNAL OF PHYSICAL CHEMISTRY · SEPTEMBER 1990

Impact Factor: 2.78 · DOI: 10.1021/j100381a032

2 AUTHORS:

Yannis G. Lazarou
National Center for Scientific Research Demo…
43 PUBLICATIONS **551** CITATIONS
SEE PROFILE

Panos Papagiannakopoulos
University of Crete
66 PUBLICATIONS **656** CITATIONS
SEE PROFILE

Infrared Multiphoton Decomposition of Dimethylnitramine

Yannis G. Lazarou and Panos Papagiannakopoulos*

Department of Chemistry, University of Crete, and Institute of Electronic Structure and Laser, Research Center of Crete, P.O. Box 1470, Heraklion 714 09, Crete, Greece *(Received: January 5, 1990)*

The infrared multiphoton dissociation of dimethylnitramine in the gas phase by a pulsed CO_2 laser has been studied in order to elucidate its photochemical decomposition mechanism under collisionless conditions and provide a qualitative understanding of the consequent chemical mechanism that leads to the final products. The experimentally determined steady-state rate coefficient for the unimolecular decomposition of dimethylnitramine was found to be $k(\mathrm{st}) = 10^{5.5\pm0.1}(I/\mathrm{MW\ cm^{-2}})\ \mathrm{s^{-1}}$ for laser intensities 2-10 MW $\mathrm{cm^{-2}}$. Scavenging experiments with Cl_2, NOCl, NO, NO_2, and $(CD_3)_2NNO_2$ molecules have shown that the decomposition dynamics proceeds through scission of the N-NO_2 bond, with no evidence of the HONO elimination or the isomerization to nitro-nitrite channel. Dimethylnitrosamine was the major final product which was mainly produced through oxidation of dimethylamino radical by dimethylnitramine.

Introduction

The thermal decomposition of nitro compounds in the gas phase is a complex chemical process with considerable interest and applications in the propellant industry. In general, nitro compounds are thermally unstable molecules consisting of relatively weak covalent bonds (N-N, O-N, C-N), which are easily broken, yielding highly reactive intermediate species. In particular, the thermal stability of the nitramine functional group NNO_2 is of great interest, since it is contained in many energetic molecules (RDX, HMX, etc) and plays a significant role in the complex mechanism of their thermal decomposition. *N,N*-Dimethylnitramine (DMNA) is the simplest dialkylnitramine and its thermal decomposition kinetics in the gas phase has been studied initially by two investigations.[1,2] In both experiments, the main products of dimethylnitramine pyrolysis were *N,N*-dimethylnitrosamine (DMNO) and nitric oxide and the proposed formation mechanism included the following reactions:

$$(CH_3)_2NNO_2 \rightarrow (CH_3)_2N + NO_2 \quad (I)$$

$$(CH_3)_2NNO_2 + NO_2 \rightarrow NO + \text{oxidation products} \quad (II)$$

$$(CH_3)_2N + NO \rightarrow (CH_3)_2NNO \quad (III)$$

In this scheme dimethylnitramine molecules are initially decomposed to dimethylamino radical and nitrogen dioxide by simple bond scission of the weakest N-NO_2 bond, and subsequently the dimethylamino radical recombines with nitric oxide which is formed by the reaction of nitrogen dioxide with parent dimethylnitramine. However, this mechanism is incomplete since the rate constant of the oxidation reaction (II) is unknown, although it is considered as the rate-determining step of the overall process. Furthermore, the thermal decomposition of dimethylnitramine has been studied at low temperatures (466-524 K) in static cell experiments and at high temperatures (800-1000 K) in shock tubes.[3] The activation energy of the overall process was found to be 22 kcal/mol and dimethylnitrosamine was the main product of decomposition. The dimethylnitrosamine formation was also explained through reaction (III), and the primary source of NO was the decomposition of CH_3NO which was formed by the four-center elimination reaction:

$$(CH_3)_2N + NO_2 \rightarrow 2CH_3NO \quad (IV)$$

More recent laser pyrolysis experiments in a VLPR system[4] have shown that, besides the main N-NO_2 bond fission channel of decomposition, a substantial fraction of dimethylnitramine molecules isomerize to N-nitrite and subsequently decompose through fission of the NO-NO bond.

The infrared multiphoton decomposition (IRMPD) of polyatomic molecules is a powerful technique[5] for studying the energetics and dynamics of unimolecular dissociation processes, since it overcomes the complications of secondary dissociation processes occurring in pyrolysis experiments. This is mainly due to the selective and controlled infrared multiphoton absorption (IRMPA) process, which provides vibrational energy specifically to the parent molecules (usually leaving the dissociation products intact) and results in desirable levels of vibrational excitation depending on the laser intensity.[6-8] In addition, due to the fast intramolecular vibrational relaxation (IVR) occurring in vibrationally excited polyatomic molecules, statistical theories of unimolecular decomposition (like RRKM[9]) can be employed to provide an understanding of the dissociation process and an interpretation of the experimental results.

In this work we study the IRMPD of dimethylnitramine using a tunable pulsed CO_2 laser. It is important to determine the primary channel of unimolecular decomposition and elucidate the reaction mechanism that results in the final products. This is done by chemical trapping of the primary photofragments with various added gaseous scavengers and subsequently detecting the final products with a mass spectrometer.

Experimental Section

The IR photolysis experiments were performed with a tunable TEA CO_2 laser (Lumonics Model 103-2) with a relatively constant energy density beam. The energy of the laser pulse was measured with a calibrated thermopile (Lumonics Model 20D) and was in the range 3-7 J at 971.9 $\mathrm{cm^{-1}}$ [R(14) line at the 10.6-μm band]. The transverse profile of the beam was Gaussian with fwhm = 21 mm, while the horizontal profile was almost square with fwhm = 32 mm. Therefore, the laser beam cross section was 7 $\mathrm{cm^2}$. The laser pulse duration was recorded with a photon drag detector (Rofin 7441) and consisted mainly of a 80-ns spike followed by a 600-ns minor tail (10%).

The photolysis experiments were performed in the gas phase in a Pyrex cell of 4 cm diameter and 17 cm length with NaCl windows. The laser beam was transmitted unfocused through the

(1) Flournoy, J. M. *J. Chem. Phys.* **1962**, *36*, 1106.
(2) Korsunskii, B. L.; Dubovitskii, F. I. *Dokl. Akad. Nauk. SSSR* **1964**, *155*, 402.
(3) Lloyd, S. A.; Umstead, M. E.; Lin, M. C. *J. Energetic Mater.* **1985**, *3*, 187.
(4) (a) Nigenda, S. E.; McMillen, D. F.; Golden, D. M. *J. Phys. Chem.* **1989**, *93*, 1124. (b) Stewart, P. M.; Jeffries, J. B.; Zellweger, J. M.; Golden, D. M.; McMillen, D. F. *J. Phys. Chem.* **1989**, *93*, 3557.
(5) Wodtke, A. M.; Hintsa, E. J.; Lee, Y. T. *J. Phys. Chem.* **1986**, *90*, 3549.
(6) Ambartzumian, R. V.; Letokhov, V. S. In *Chemical and Biochemical Applications of Lasers*; Moore, C. B., Ed.; Academic Press: New York, 1977; Vol. III, p 167.
(7) Cantrell, C. P.; Freund, S. M.; Lyman, J. L. In *Laser Handbook*; Stitch, M. L., Ed.; North-Holland: Amsterdam, 1979; Vol. III, p 485.
(8) Schulz, P. A.; Sudbo, Aa. S.; Krajnovitch, D. J.; Kwok, J. S.; Shen, Y. R.; Lee, Y. T. *Annu. Rev. Phys. Chem.* **1979**, *30*, 379.
(9) Robinson, P. J.; Holbrook, K. A. *Unimolecular Reactions*; Wiley: London, 1972.

0022-3654/90/2094-7114$02.50/0

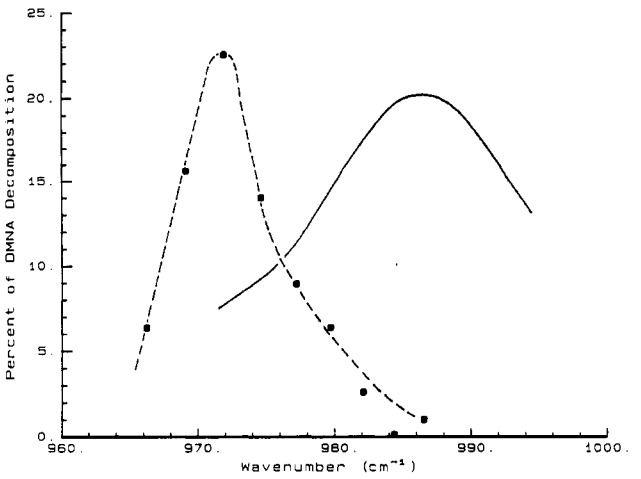

Figure 1. The frequency dependence of the IRMPD yield of dimethylnitramine versus the linear absorption spectrum (solid line). [DMNA] = 100 mTorr, at laser fluence 0.3 J cm^{-2} after 200 pulses.

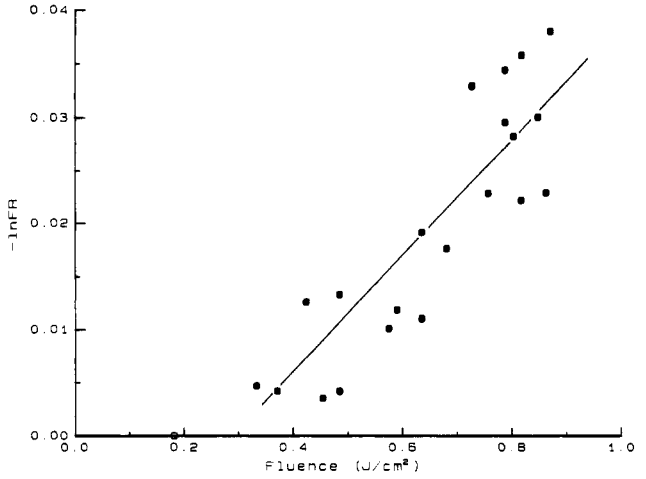

Figure 2. The yield function $-\ln F_R$ versus the laser fluence, and the least-squares fit to the data. [DMNA] = 100 mTorr; yields after 50 pulses irradiation at 971.9 cm^{-1}.

reaction cell and was selectively attenuated with polyethylene sheets. The partial pressure of the sample gases was measured with calibrated transducer gauges (Validyne DP15).

The chemical analysis of the gaseous samples was performed before and after photolysis with a quadrupole mass spectrometer (Balzers QMG 511). The samples were introduced to the ionizer, placed in a high vacuum of 10^{-7} Torr, through a 1 mm diameter stainless steel tubing, and the flow was controlled with a fine metering valve. At an electron energy of 70 eV, dimethylnitramine showed fragments at m/e 90 parent (0.32), 74 (0.04), 44 (0.22), 43 (0.72), 42 (1.00), 30 (0.20), 28 (0.42), 18 (0.73), and 15 (0.44), while dimethylnitrosamine at m/e 74 parent (1.00), 44 (0.07), 43 (0.45), 42 (1.00), 30 (0.30), 28 (0.59), 18 (0.30), and 15 (0.80) in agreement with previous experiments.[10] The acquisition and correction of the mass spectra was carried out with a PDP-11/23 microprocessor running home-made application software, interfaced to the quadrupole mass spectrometer. The raw digitized mass spectra were corrected first by subtracting the background contribution and then by considering the fragmentation pattern of the involved species. Therefore, mass spectra of all interesting species were obtained in a digital form and stored in a spectra library. The uncertainty in estimating the intensity of the mass peaks was less than 10% and the experimental error in estimating the ratio of various mass peaks was less than 15%. Thus, the observed behavior of the various ratios as a function of added gas concentration was not affected by the experimental error.

The dimethylnitramine and dimethylnitramine-d_6 were synthesized by nitration of the corresponding dialkylformamide[11] and were further purified by subsequent degassing. All gases used, except NOCl which was synthesized, were of high purity (Linde 2.8) and were also degassed under vacuum prior to use.

Results

1. Laser-Induced Decomposition of $(CH_3)_2NNO_2$. Experiments were performed by irradiating dimethylnitramine at 971.9 cm^{-1} [10R(14) laser line], which lies 15 cm^{-1} red-shifted from the CH_3-rocking absorption band at 987 cm^{-1}.[12] The dimethylnitramine pressure was around 100 mTorr so that IRMPD was almost collisionless. The decomposition yield was also linear with the number of laser pulses up to 80 and for laser fluences less than 0.8 J cm^{-2}; therefore, most experiments were performed with 50 pulses. Secondary photolysis of dimethylnitrosamine was not present in our experiments, since unfocused photolysis experiments of dimethylnitrosamine at 971.93 cm^{-1} showed no appreciable decomposition.

At first, the frequency dependence of the total decomposition yield of dimethylnitramine was studied and the experimental data are shown in Figure 1. The laser fluence was adjusted and fixed at approximately 0.3 J cm^{-2} for the laser lines R(6) to R(38) of the 10.6-μm band. The linear absorption spectrum of 250 mTorr of dimethylnitramine was taken in a 8-cm cell with an FT-IR spectrometer. The change in the decomposition yield of dimethylnitramine with the CO_2 laser frequency follows approximately the same shape as in the linear absorption spectrum, although the maximum in the IRMPD spectrum is shifted to the red compared to the one-photon absorption curve.

The dependence on laser fluence of the remaining fraction of dimethylnitramine molecules $F_R = [DMNA]_f/[DMNA]_0$ was also studied at 971.9 cm^{-1} [10R(14) laser line] and the experimental data are shown in Figure 2. The yield function $-\ln F_R$ rises linearly with the laser fluence and the least-squares fit to the data provides the slope, which gives the steady-state rate coefficient for dimethylnitramine unimolecular decomposition

$$k(\mathrm{st}) = 10^{5.5\pm0.1}(I/\mathrm{MW\ cm^{-2}})\ \mathrm{s^{-1}}$$

for laser intensity range I = 3–10 MW cm^{-2}.[13] The horizontal axis intersection provides the threshold laser fluence for decomposition which was found to be 0.28 J cm^{-2}. The error limit is a factor of 2 and includes systematic errors and possible deviations from the model functions.

The final gaseous products of CO_2 laser-induced decomposition of dimethylnitramine were dimethylnitrosamine (DMNO), *N*-methylmethylenimine (CH_2=NCH_3), formaldoxime (CH_2=N-OH), nitric oxide, nitrogen dioxide, and tetramethylhydrazine. Their yields were determined by measuring the intensity of the parent and/or fragments mass peaks. Therefore, dimethylnitrosamine was determined by the m/e 74 parent peak, *N*-methylmethylenimine by the m/e 43 and 42 parent and fragment peaks, formaldoxime by the m/e 45 parent peak, and tetramethylhydrazine by the m/e 88 parent peak. The m/e 45 mass peak was assigned to formaldoxime instead of nitrosomethane, since upon deuteration of surfaces a new peak appears at m/e 46 corresponding to CH_2N=OD with simultaneous decrease of the m/e 45 peak. Although a detailed mass balance analysis was not possible, it was found that around 65% of the decomposed dimethylnitramine could be accounted for, appearing as dimethylnitrosamine (~55%) and formaldoxime (~15%). *N*-Methylmethyleneimine, tetramethylhydrazine, nitric oxide, and nitrogen dioxide were also identified as products but their yields could not be determined.

2. Laser-Induced Decomposition of $(CH_3)_2NNO_2$ *in the Presence of Various Scavenging Gases.* Experiments were also performed by irradiating 100 mTorr of dimethylnitramine at 971.9

(10) Bulusu, S.; Axenrod, T.; Milne, G. W. A. *Org. Mass. Spectrom.* **1970**, *3*, 13.
(11) Robson, J. H. *J. Am. Chem. Soc.* **1955**, *77*, 107.
(12) Trinquecoste, C.; Rey-Lafon, M.; Forel, M. *Spectrochim. Acta* **1974**, *30*, 813.
(13) Quack, M.; Seyfang, G. *J. Chem. Phys.* **1982**, *76*, 955.

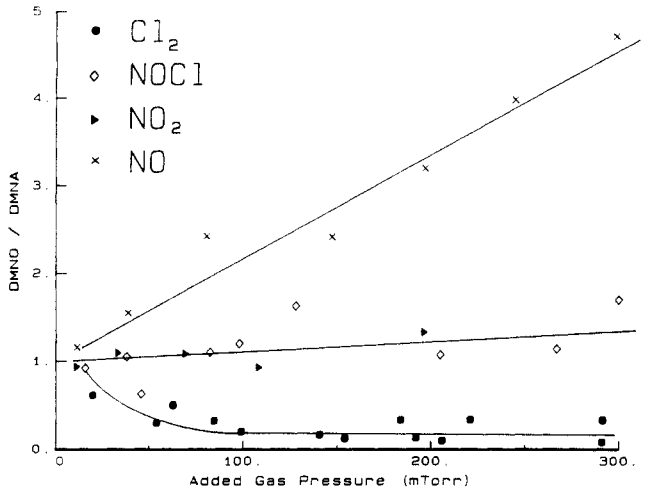

Figure 3. The $[DMNO]/[DMNA]_f$ ratio versus pressure of added scavenging gases, Cl_2, NO, NOCl, and NO_2. [DMNA] = 100 mTorr, after 50 pulses irradiation at 971.9 cm^{-1} with 0.8 J cm^{-2} laser fluence.

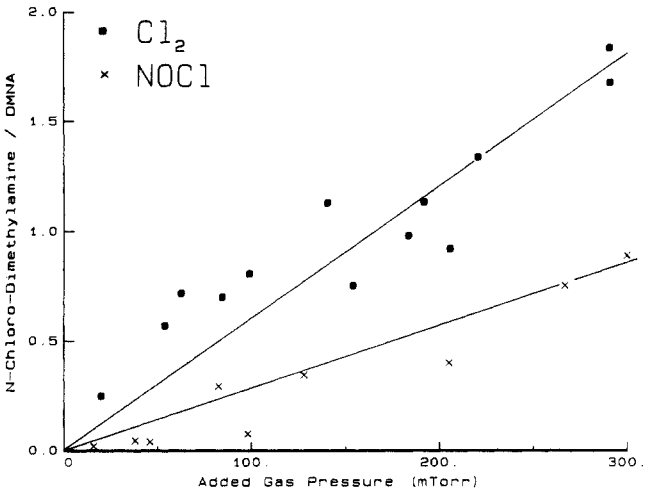

Figure 4. The $[(CH_3)_2NCl]/[DMNA]_f$ ratio versus pressure of added scavenging gases Cl_2 and NOCl. [DMNA] = 100 mTorr, after 50 pulses irradiation at 971.9 cm^{-1} with 0.8 J cm^{-2} laser fluence.

cm^{-1} [10R(14) laser line] in the presence of Cl_2, NOCl, NO, NO_2, and $(CD_3)_2NNO_2$ which act as free-radical scavengers. The formation of the different final products and the dependence on the concentration of each scavenging gas were studied by mass spectrometric analysis. In particular, the ratios $[DMNO]/[DMNA]_f$, $[(CH_3)_2NCl]/[DMNA]_f$, $[CH_2{=}NOH]/[DMNA]_f$, and $[NO_2]/[DMNA]_f$ were determined as a function of added gas concentration.

(a) The addition of chlorine induced a drastic decrease in dimethylnitrosamine, formaldoxime, and tetramethylhydrazine formation and a sharp increase in $(CH_3)_2NCl$ and NO_2 production. The *N*-chlorodimethylamine molecules were detected by their *m/e* 79 and 81 parent peaks (both chlorine isotopes). The dimethylnitrosamine formation decreased exponentially with chlorine concentration, Figure 3, while the *N*-chlorodimethylamine and NO_2 increased almost linearly with the chlorine concentration, Figures 4 and 5, respectively.

(b) The addition of nitrosyl chloride resulted in a simultaneous increase in *N*-chlorodimethylamine and NO_2 formation and a decrease in tetramethylhydrazine and formaldoxime production. The dimethylnitrosamine formation showed a minor increase with NOCl concentration, Figure 3, while the NO_2 production increased linearly with NOCl concentration as in the case of added chlorine, Figure 5. The *N*-chlorodimethylamine formation was almost linear with NOCl concentration with a slower rate than with chlorine concentration, Figure 4.

(c) The addition of nitric oxide induced a sharp increase in dimethylnitrosamine formation and a minor increase in NO_2 production. The dimethylnitrosamine formation increased linearly with NO concentration, Figure 3, while the formaldoxime production did not show any major increase, Figure 6.

(d) The addition of nitrogen dioxide did not produce any change in the dimethylnitrosamine/dimethylnitramine ratio, Figure 3. The formaldoxime yield increased with NO_2 concentration up to 80 mTorr and then appeared to decrease, Figure 6.

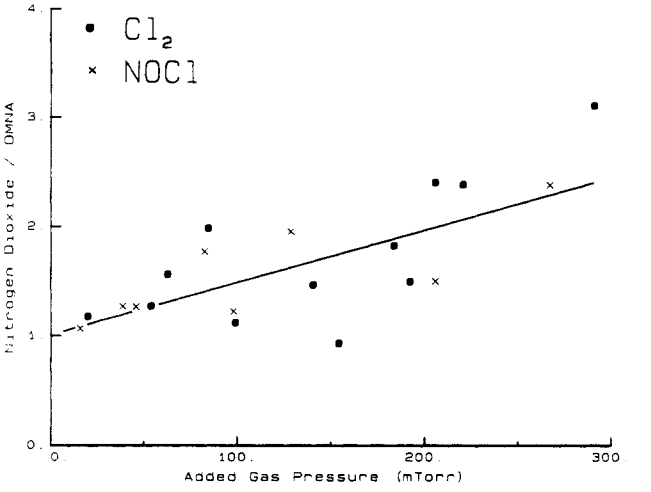

Figure 5. The $[NO_2]/[DMNA]_f$ ratio versus pressure of added scavenging gases Cl_2 and NOCl. [DMNA] = 100 mTorr, after 50 pulses irradiation at 971.9 cm^{-1} with 0.8 J cm^{-2} laser fluence.

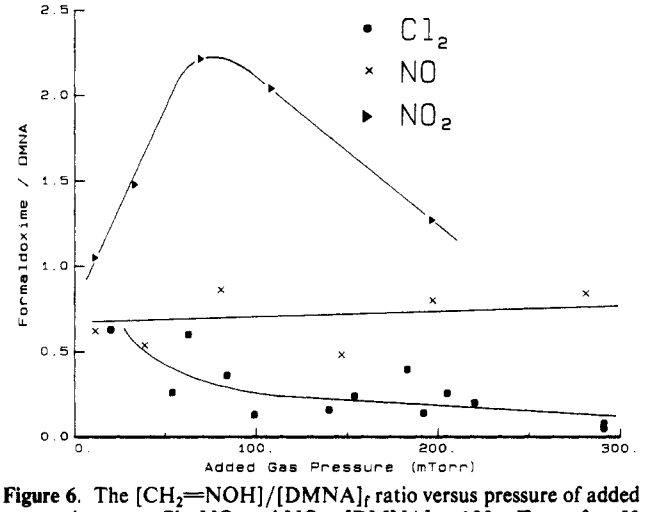

Figure 6. The $[CH_2{=}NOH]/[DMNA]_f$ ratio versus pressure of added scavenging gases Cl_2, NO, and NO_2. [DMNA] = 100 mTorr, after 50 pulses irradiation at 971.9 cm^{-1} with 0.8 J cm^{-2} laser fluence.

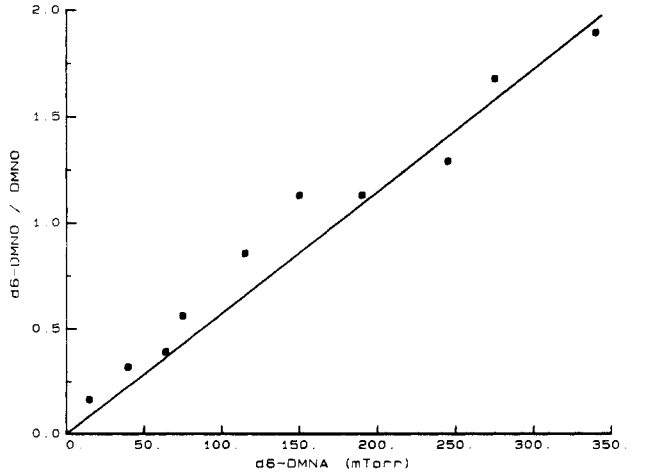

Figure 7. The $[DMNO\text{-}d_6]_f/[DMNO]_f$ ratio versus DMNA-d_6 pressure. [DMNA] = 200 mTorr, after 50 pulses irradiation at 971.9 cm^{-1} with 0.8 J cm^{-2} laser fluence.

(e) The addition of perdeuteriodimethylnitramine resulted in the formation of $(CD_3)_2NNO$ and the ratio [DMNO-d_6]/[DMNO] increased almost linearly with $(CD_3)_2NNO_2$ concentration, Figure 7. $(CD_3)_2NNO_2$ did not absorb the CO_2 laser radiation since the CD_3-rocking absorption band is shifted to 880 cm^{-1}. There was also no formation of $(CD_3)_2NN(CD_3)_2$ and $(CH_3)_2NN(CD_3)_2$.

Discussion

The observed dimethylnitramine decomposition induced by the CO_2 laser radiation is a purely photochemical process, since the overall decomposition yield depends on the laser frequency. No decomposition is observed upon irradiation at laser frequencies away from the CH_3-rocking absorption band of dimethylnitramine. The observed red shift ($\sim$15 cm^{-1}) in the IRMPD spectrum relative to its linear absorption spectrum is normal as in most polyatomic molecules.[6] Furthermore, the laser fluence dependence provides the range for the unimolecular decomposition rate constant $k_{uni} = (0.9–3.2) \times 10^6$ s^{-1} for laser intensities I = 3–10 MW cm^{-2}, respectively. The estimated overall dimethylnitramine disappearance is mainly due to its unimolecular decomposition with minor contribution from radical–dimethylnitramine reaction ($k_3 \sim 10^{10}$ L mol^{-1} s^{-1}),[14] since the concentrations were low. Finally, the unimolecular decomposition of dimethylnitramine can be considered as collisionless at low pressures ($\sim$100 mTorr), since the decomposition half-life (τ = 0.3–1 μs) is shorter than the mean collision time ($\sim$1 μs), and the laser pulse duration is 80 ns.

Our experimental results suggest that the unimolecular decomposition of dimethylnitramine proceeds through scission of the N–NO_2 bond

$$(CH_3)_2NNO_2 \rightarrow (CH_3)_2N + NO_2 \qquad \Delta H°_{300} = +46.5 \text{ kcal/mol} \quad (1)$$

This is clearly shown in the experiments with chlorine addition, where the dimethylamino radical is scavenged very efficiently through reaction

$$(CH_3)_2N + Cl_2 \rightarrow (CH_3)_2NCl + Cl \qquad \Delta H°_{300} = -12 \text{ kcal/mol} \quad (2)$$

to yield N-chlorodimethylamine molecules. Simultaneously, the other primary photofragment, NO_2, appears also as a major final product. Furthermore, an increase in chlorine concentration results in a drastic increase in N-chlorodimethylamine and NO_2 formation and a sharp decrease in dimethylnitrosamine, formaldoxime, and tetramethylhydrazine yield. Such behavior suggests that the last three products are induced by dimethylamino radical reactions. In particular, dimethylnitrosamine is mainly produced by the oxygen abstraction reaction

$$(CH_3)_2N + (CH_3)_2NNO_2 \rightarrow (CH_3)_2NO + (CH_3)_2NNO \qquad \Delta H°_{300} = -11 \text{ kcal/mol} \quad (3)$$

and tetramethylhydrazine by the recombination reaction

$$(CH_3)_2N + (CH_3)_2N \rightarrow (CH_3)_2NN(CH_3)_2 \qquad \Delta H°_{300} = -49 \text{ kcal/mol} \quad (4)$$

The mechanism of formaldoxime formation is less certain but it appears to occur through β-scission of the relatively stable nitroxyl radical and subsequent isomerization of nitrosomethane

$$(CH_3)_2NO \rightarrow CH_3NO + CH_3 \quad (5)$$

$$CH_3NO \rightarrow CH_2{=}NOH \quad (6)$$

The presence of reaction 3 is unequivocally shown in the experiments with dimethylnitramine-d_6 addition, where the dimethylnitrosamine-d_6 formation increases with dimethylnitramine-d_6 concentration. Furthermore, equal dimethylnitramine and dimethylnitramine-d_6 concentrations lead to equal amounts of corresponding dimethylnitrosamines. The absence of any $(CD_3)_2NN(CD_3)_2$ and $(CH_3)_2NN(CD_3)_2$ formation proves that dimethylnitramine-d_6 does not decompose (photochemically or thermally) along the N–N bond yielding dimethylamino-d_6 radicals. Therefore, the formation of dimethylnitrosamine-d_6 occurs mainly through oxidation reaction 3, rather than through recombination of dimethylamino-d_6 radical with NO.

The experiments with NOCl, NO, and NO_2 addition are also in agreement with the above analysis. The addition of NOCl promotes the parallel reactions

$$(CH_3)_2N + NOCl \rightarrow (CH_3)_2NCl + NO \qquad \Delta H°_{300} = -32 \text{ kcal/mol} \quad (7)$$

$$(CH_3)_2N + NOCl \rightarrow (CH_3)_2NNO + Cl \qquad \Delta H°_{300} = -7 \text{ kcal/mol} \quad (8)$$

yielding N-chlorodimethylamine and dimethylnitrosamine. The increase in NOCl concentration results in higher yields of N-chlorodimethylamine and dimethylnitrosamine. The presence of reaction 8 is also apparent from the slower rate of N-chlorodimethylamine formation with NOCl than with chlorine concentration. The addition of NO enhances the formation of dimethylnitrosamine through the reaction

$$(CH_3)_2N + NO \rightarrow (CH_3)_2NNO \qquad \Delta H°_{300} = -45 \text{ kcal/mol} \quad (9)$$

On increasing the NO concentration, a sharp increase in the dimethylnitrosamine formation is observed due to the above recombination reaction 9, while the formaldoxime yield remains invariable, indicating that the main route of its formation is the oxidation reaction 3. The addition of NO_2 promotes the formation of formaldoxime through oxidation reaction

$$(CH_3)_2N + NO_2 \rightarrow (CH_3)_2NO + NO \qquad \Delta H°_{300} = -13 \text{ kcal/mol} \quad (10)$$

that may compete with the recombination reaction

$$(CH_3)_2N + NO_2 \rightarrow (CH_3)_2NNO_2 \qquad \Delta H°_{300} = -46.5 \text{ kcal/mol} \quad (11)$$

However, at higher NO_2 concentrations the observed formaldoxime yield decreases due to the secondary reaction of formaldoxime with NO_2. This reaction has been observed to proceed very rapidly at room temperature.

Our experimental results do not indicate the presence of the isomerization channel of dimethylnitramine that is reported by recent thermal experiments.[4] This channel should proceed through the reactions

$$(CH_3)_2NNO_2 \rightarrow (CH_3)_2NONO \rightarrow (CH_3)_2NO + NO \quad (12)$$

and lead to dimethylnitroxyl radical formation which according to our experimental results is converted to formaldoxime. However, the addition of chlorine even at high concentrations did not produce any formaldoxime and NO that could be accounted for by the isomerization channel.

From the thermochemical point of view, the most probable unimolecular decomposition channels of dimethylnitramine are (a) the scission of the weak N–NO_2 bond, (b) the five-center HONO elimination, and (c) the isomerization to $(CH_3)_2NONO$ followed by scission of the NO–NO bond. Reaction enthalpy, estimated preexponential, and threshold energy values for these channels are presented in Table I. Other single-bond-scission processes are expected to be less competitive since their dissociation energies are much higher: N–O (90), C–N (92), and C–H (90) estimated bond energies (kcal/mol).[15,16] This analysis is in agreement with our experimental results since the N–NO_2 bond scission channel is faster than the other two pathways. Classical trajectory calculations have also shown that the NO_2 elimination is the predominant dissociation pathway and that the vibrational

(14) Slagle, I. R.; Gutman, D. *J. Am. Chem. Soc.* **1982**, *104*, 4741.

(15) Benson, S. W. *Thermochemical Kinetics*; 2nd ed.; Wiley-Interscience: New York, 1976.

(16) Melius, C. F.; Binkley, J. S. Thermochemistry of the Decomposition of Nitramines in the Gas Phase. *Twenty-first Symposium (International) on Combustion, [Proceedings]*; The Combustion Institute; Pittsburgh, 1986; p 1953.

TABLE I: Fundamental Vibrational Frequencies (cm^{-1}) and Degeneracies (in Parentheses) of Ground State and the Transition States of $(CH_3)_2NNO_2$ Molecule

		transition states		
	ground state	N–N fission	HONO elimn	isomerizn
C–H str	2940 (6)		2000	
N–O	1560			
H–C–H bend	1430 (4)		1000	
N–O str	1300		1200	1500
N–N str	1250	rc	690	690
C–N–C bend	1200	840		
H–C–N bend	1150 (6)	800 (6)	800	
C–N str	1100 (2)		1430	
C–N–N bend	800 (2)	560 (2)		600
N–N–O bend	640 (3)	450 (3)	830	450
C–N torsion	230 (2)	160 (2)	460	
N–N torsion	150	50	rc	rc
E_z, kcal/mol	59.5	52.7	57.6	58.6
E_0, kcal/mol		46.5[a]	42.5[b]	40
I^*/I	1	6	1	1.5
σ, n	2, 1	2, 1	1, 1	1, 2
ΔH_0, kcal/mol		46.5[a]	2.8[c]	28.5[d]
log A/s^{-1}		15.5	12.7	13.3

[a] Recommended value.[4a] [b] Assumed as for nitroethane and 2-nitropropane.[5] [c] Based on estimated $\Delta H_f°(CH_3—N=CH_2)$ = 17.3 kcal/mol. [d] Based on extrapolated $\Delta H_f°((CH_3)_2NONO)$ = 24.4 kcal/mol from similar amino nitrites.[16]

energy flows rapidly (within 0.25 ps) and irreversibly from the methyl groups into the nitro group.[17]

Our experimental results are in substantial agreement with the molecular beam IRMPD study of Wodtke and Lee (private communication quoted in ref 4) but there is a major difference between IRMPD and laser-powered pyrolysis (true thermal decomposition, ref 4) in that the nitro–nitrite rearrangement occurs only under the latter conditions. This disagreement may be due to the fact that the two methods produce different degrees of vibrational excitation above the dissociation limit. The laser pyrolysis experiments were performed within an estimated temperature 900 K, while the IRMPD experiments were performed within an effective temperature range 1060–1250 K, since the decomposition rates were $k_{uni} = 10^6$–$10^{6.5}$ s^{-1} and the N–N bond scission was the primary pathway. Calculations of the unimolecular rate constant k as a function of internal energy E for the three major channels of decomposition were done by using the RRKM theory and Whitten–Rabinovitch approximation[9] and are presented in Figure 8. The vibrational frequencies, the zero-point energy E_z, the critical energy E_0, the total moment of inertia ratio I^*/I, the symmetry number, and the optical isomer number for ground and transition states[12] are included in Table I. Assuming that the activation energy for the nitro–nitrite rearrangement pathway is around 40 kcal/mol, the branching ratio k_{N-N}/k_{isom} is given by the expression $10^{2.2}\exp(-6.5/RT)$. Therefore, in the laser pyrolysis experiments where the temperature is 900 K the branching ratio is higher than 4 and the nitro–nitrite rearrangement represents more than 20% of the total dimethylnitramine decomposition. On the contrary, in the IRMPD experiments where the effective temperature is higher, ~1150 K, the branching ratio becomes almost 10 and the nitro–nitrite rearrangement pathway is limited to less than 10% of the total decomposition and therefore very difficult to detect with our method. From Figure 8, the experimentally obtained decomposition rate constants $k_{uni} = 10^6$–$10^{6.5}$ s^{-1} for the applied laser intensities correspond to an excitation energy distribution of dissociating dimethylnitramine molecules along the N–N scission pathway with a mean energy $E^* = 56$–62 kcal/mol, respectively. Therefore, dimethylnitramine molecules are on the average pumped up to 9–15 kcal/mol above the dissociation threshold before the dissociation rates start competing with the up-pumping rate. Similar

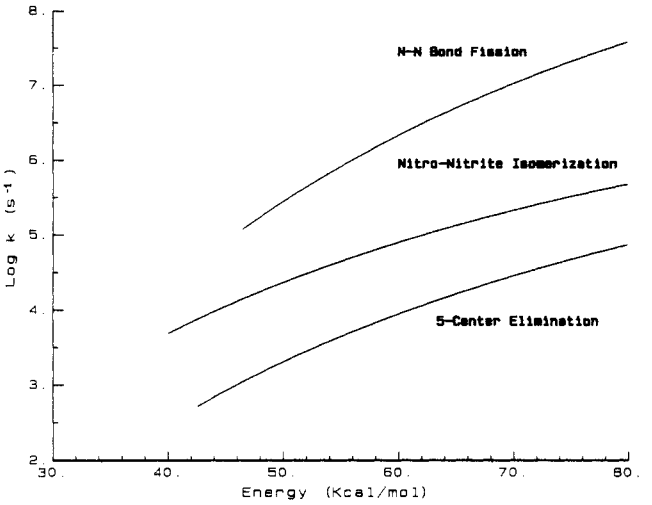

Figure 8. The RRKM calculated plots of log k_{uni} versus energy.

degree of vibrational excitation above the dissociation limit has been observed in IRMPE of nitroalkanes.[5] At this level of excitation the other two decomposition pathways are noncompetitive. However, in KrF laser induced decomposition experiments of dimethylnitramine and hexahydro-1,3,5-trinitro-1,3,5-triazine (RDX),[18] it has been shown that N–N bond scission and HONO elimination pathways are competitive.

The overall chemical mechanism that follows dimethylnitramine photodissociation and is responsible for the formation of the observed final products is rather complicated. However, our qualitative analysis has shown that the oxidation reaction of dimethylamino radical

$$(CH_3)_2N + (CH_3)_2NNO_2 \rightarrow (CH_3)_2NO + (CH_3)_2NNO \quad (3)$$

is the main secondary reaction leading to dimethylnitrosamine formation, followed by the unimolecular processes

$$(CH_3)_2NO \rightarrow CH_3NO + CH_3$$

$$CH_3NO \rightarrow CH_2{=}NOH$$

Moreover, the abstraction and recombination reactions of dimethylamino radical

$$(CH_3)_2N + NO_2 \rightarrow (CH_3)_2NO + NO \quad (10)$$

$$(CH_3)_2N + NO_2 \rightarrow (CH_3)_2NNO_2 \quad (11)$$

$$(CH_3)_2N + (CH_3)_2N \rightarrow (CH_3)_2NN(CH_3)_2 \quad (4)$$

$$(CH_3)_2N + (CH_3)_2N \rightarrow (CH_3)_2NH + CH_3N{=}CH_2 \quad (13)$$

are also occurring with a competitive rate. The branching ratio k_4/k_{13} of the above reaction has been found to be 1.55 ± 0.2 at room temperature.[19] Although the presence of dimethylamine is not certain due to detection difficulties, it is known to undergo rapid heterogeneous reaction with NO_2 to form dimethylnitrosamine.[20] Therefore, this nitrosation reaction must tentatively be included in the mechanism.

A quantitative analysis of the above mechanism requires knowledge of the chemical reactivity of dimethylamino radical with NO_2, NO, and dimethylnitramine. The oxidation reaction 3 is expected to have a low activation energy and a rate constant $k_3 \sim 10^{10}$ L mol^{-1} s^{-1}.[15] The recombination reactions 9 and 11 have been found to have a relative ratio $k_{11}/k_9 \sim 4$ at room

(17) Sumpter, B. G.; Thompson, D. L. *J. Chem. Phys.* **1987**, *86*, 3301.

(18) Capellos, C.; Papagiannakopoulos, P.; Liang, Y. *Chem. Phys. Lett.* **1989**, *164*, 533.

(19) Seetula, J.; Kalliorinne, K.; Koskikallio, J. *J. Photochem. Photobiol.* **1988**, *43*, 31.

(20) Hanst, P. L.; Spence, J. W.; Miller, M. *Environ. Sci. Technol.* **1977**, *11*, 403.

temperature.[21] Finally, the chemical reactivity of dimethylamino radical with NO, NO_2 and dimethylnitramine is currently under investigation with the VLPR (very low pressure reactor) technique in order to obtain their rate constants and establish their reaction pathways.

Conclusions

The infrared multiphoton dissociation of dimethylnitramine has been found to occur through scission of the weak N-NO_2 bond. The steady-state rate of decomposition has been estimated at various laser intensities and the average degree of laser excitation of dimethylnitramine molecules was $\sim 12 \pm 3$ kcal/mol above the dissociation limit. Dimethylamino radical is the primary photofragment, undergoing mainly oxidation from parent dimethylnitramine molecules, leading to the two most important decomposition products, dimethylnitrosamine and formaldoxime. This oxidative reaction is very essential to the overall mechanism of dimethylnitramine decomposition and, furthermore, to the thermal degradation of nitramines. In general, amino radicals are primary decomposition products of nitramines and act as inhibitors of similar oxidation reactions that lead to their deterioration. Our results reveal also the presence of competing secondary reactions following the photodecomposition of dimethylnitramine. A complete understanding of their thermal or photochemical decomposition, especially in the case of more complex members of the series, will require knowledge of the detailed chemical kinetics and reaction dynamics of similar amino radical reactions. Finally, such studies provide valuable information about the nitramine decomposition chemistry and the thermal stability of energetic compounds.

Acknowledgment. This work was partly supported by the University of Crete Research Committee. Y.L. also acknowledges the support by the Zervas Foundation, Athens.

(21) Lindley, C. R. C.; Calvert, J. G.; Shaw, J. H. *Chem. Phys. Lett.* **1979**, *67*, 57.

Shock Tube Study of the Reaction H + O_2 → OH + O Using OH Laser Absorption

David A. Masten,* Ronald K. Hanson, and Craig T. Bowman

High Temperature Gasdynamics Laboratory, Department of Mechanical Engineering, Stanford University, Stanford, California 94305 *(Received: January 10, 1990; In Final Form: April 17, 1990)*

Mixtures of hydrogen and oxygen dilute in argon were heated by both incident and reflected shock waves to measure the rate coefficient of the H_2/O_2 mechanism branching reaction H + O_2 → OH + O (2) in the temperature range 1450–3370 K. Time histories of OH($X^2\Pi$) were monitored by using narrow-line-width laser absorption at 306.7 nm. A detailed kinetic analysis of the data in rich mixtures yielded the following rate coefficient expression: $k_2 = (9.33 \pm 0.40) \times 10^{13} \exp[-(14800 \pm 170)$ cal mol$^{-1}/RT$, K] cm^3 mol^{-1} s^{-1}. In addition, H atom production was measured with atomic resonance absorption spectroscopy (ARAS) in incident shock experiments over the temperature range 1450–2152 K both simultaneously with OH detection and in separate experiments. The rate coefficient data obtained by ARAS are in excellent agreement with those based on the OH absorption but exhibit larger scatter. The rate coefficient derived from OH measurements lies 27–38% below the determination of Frank and Just (1985) at 1700–2500 K and agrees with that of Pirraglia et al. (1989), within their stated uncertainty, at overlapping temperatures of 1450–1705 K.

Introduction

The chain-branching reaction H + O_2 → OH + O is one of the most important elementary gas-phase reactions in combustion. Under many conditions, it is the rate-controlling reaction in H_2/O_2 combustion, and it is also an integral part of all hydrocarbon oxidation mechanisms. Since the review of Baulch et al.,[1] it has been the subject of numerous high-temperature experimental investigations,[2-9] theoretical studies,[10-12] and subsequent reviews.[13-15] The near factor of 2 discrepancy in these recent experimental and theoretical studies is significant due to the sensitivity of ignition and flame propagation to this reaction.

With the advent of CW ring dye lasers as a narrow-line-width source of tunable radiation, quantitative and highly sensitive detection of several molecular radicals has become feasible in shock tube experiments.[16-20] This laser absorption approach was used here to monitor the OH concentration in the hydrogen–oxygen reaction.

The growth of the concentrations of the free radicals H, O, and OH in the H_2/O_2 reaction is primarily controlled by the chain-propagating and -branching reactions

(1) Baulch, D. L.; Drysdale, D. D.; Horne, D. G.; Lloyd, A. C. *Evaluated Data for High Temperature Reactions*; Butterworths: London, 1972; Vol. 1.
(2) Schott, G. L. *Combust. Flame* **1973**, *21*, 357.
(3) Chiang, C. C.; Skinner, G. B. *Twelfth Symposium (International) on Shock Tubes and Waves*; Magnes Press: Jerusalem, 1979; p 629.
(4) Pamidimukkala, K. M.; Skinner, G. B. *Thirteenth Symposium (International) on Shock Tubes and Waves*; SUNY Press: Albany, NY, 1980; p 585.
(5) Frank, P.; Just, Th. *Ber. Bunsen-Ges. Phys. Chem.* **1985**, *89*, 181.
(6) Fujii, N.; Shin, K. S. *Chem. Phys. Lett.* **1988**, *151*, 461.
(7) Vandooren, J.; da Cruz, F.; Nelson; Van Tiggelen, P. J. *Twenty-Second Symposium (International) on Combustion*; The Combustion Institute: Pittsburgh, 1988; p 1587.
(8) Pirraglia, A. N.; Michael, J. V.; Sutherland, J. W.; Klemm, R. B. *J. Phys. Chem.* **1989**, *93*, 282.
(9) Yuan, T.; Wang, C.; Rabinowitz, M. J.; Frenklach, M. Measurement of the Rate Coefficient of the Reaction H + O_2 → OH + O. Eastern States Section/Combustion Institute Meeting, Oct 1989.
(10) Miller, J. A. *J. Chem. Phys.* **1981**, *74*, 5120.
(11) Miller, J. A. *J. Chem. Phys.* **1986**, *84*, 6170.
(12) Troe, J. *J. Phys. Chem.* **1986**, *90*, 3485.
(13) Dixon-Lewis, G.; Williams, D. J. In *Comprehensive Chemical Kinetics*; Bamford, C. H., Tipper, C. F. H., Eds.; Elsevier: Amsterdam, 1977; Vol. 17.
(14) Warnatz, J. In *Combustion Chemistry*; Gardiner, Jr., W. C., Ed.; Springer-Verlag: New York, 1984; Chapter 5.
(15) Cohen, N.; Westberg, K. R. *J. Phys. Chem. Ref. Data* **1983**, *12*, 531.
(16) Hanson, R. K.; Salimian, S.; Kychakoff, G.; Booman, R. A. *Appl. Opt.* **1983**, *21*, 641.
(17) Louge, M. Y.; Hanson, R. K.; Rea, E. C.; Booman, R. A. *J. Quant. Spectrosc. Radiat. Transfer* **1984**, *32*, 353.
(18) Kohse-Höinghaus, K.; Davidson, D. F.; Chang, A. Y.; Hanson, R. K. *J. Quant. Spectrosc. Radiat. Transfer* **1989**, *42*, 1.
(19) Mertens, J. D.; Chang, A. Y.; Hanson, R. K.; Bowman, C. T. *Int. J. Chem. Kinet.* **1989**, *21*, 1049.
(20) Dean, A. J.; Hanson, R. K. *J. Quant. Spectrosc. Radiat. Transfer* **1989**, *42*, 375.

0022-3654/90/2094-7119$02.50/0